

This is a copy of the published version, or version of record, available on the publisher's website. This version does not track changes, errata, or withdrawals on the publisher's site.

Influence of axial mirror ratios on the kinetic instability threshold in electron cyclotron resonance ion source plasma

V. Toivanen, B. S. Bhaskar, H. Koivisto, L. Maunoury, O. Tarvainen, and T. Thuillier

Published version information

Citation: V Toivanen et al. Influence of axial mirror ratios on the kinetic instability threshold in electron cyclotron resonance ion source plasma. Phys Plasmas 29, no. 1 (2022): 013501

DOI: [10.1063/5.0069638](https://doi.org/10.1063/5.0069638)

This article may be downloaded for personal use only. Any other use requires prior permission of the author and AIP Publishing.

This version is made available in accordance with publisher policies. Please cite only the published version using the reference above. This is the citation assigned by the publisher at the time of issuing the APV. Please check the publisher's website for any updates.

This item was retrieved from **ePubs**, the Open Access archive of the Science and Technology Facilities Council, UK. Please contact epublications@stfc.ac.uk or go to <http://epubs.stfc.ac.uk/> for further information and policies.

Influence of axial mirror ratios on the kinetic instability threshold in electron cyclotron resonance ion source plasma

Cite as: Phys. Plasmas **29**, 013501 (2022); <https://doi.org/10.1063/5.0069638>

Submitted: 01 September 2021 • Accepted: 08 December 2021 • Published Online: 03 January 2022

 V. Toivanen,  B. S. Bhaskar,  H. Koivisto, et al.

COLLECTIONS

 This paper was selected as an Editor's Pick



View Online



Export Citation



CrossMark

ARTICLES YOU MAY BE INTERESTED IN

[Diagnostic techniques of minimum-B ECR ion source plasma instabilities](#)

Review of Scientific Instruments **93**, 013302 (2022); <https://doi.org/10.1063/5.0075443>

[Measuring magnetic flux suppression in high-power laser-plasma interactions](#)

Physics of Plasmas **29**, 012701 (2022); <https://doi.org/10.1063/5.0062717>

[Accelerated steady-state electrostatic particle-in-cell simulation of Langmuir probes](#)

Physics of Plasmas **29**, 013502 (2022); <https://doi.org/10.1063/5.0072994>

Physics of Plasmas

Papers from 62nd Annual Meeting of the
APS Division of Plasma Physics

Read now!



Influence of axial mirror ratios on the kinetic instability threshold in electron cyclotron resonance ion source plasma

Cite as: Phys. Plasmas **29**, 013501 (2022); doi: 10.1063/5.0069638

Submitted: 1 September 2021 · Accepted: 8 December 2021 ·

Published Online: 3 January 2022



View Online



Export Citation



CrossMark

V. Toivanen,^{1,a)}  B. S. Bhaskar,^{1,2}  H. Koivisto,¹  L. Maunoury,³  O. Tarvainen,^{1,4}  and T. Thuillier² 

AFFILIATIONS

¹Department of Physics, University of Jyväskylä (JYFL), 40500 Jyväskylä, Finland

²Univ. Grenoble Alpes, CNRS, Grenoble INP, LPSC-IN2P3, 38000 Grenoble, France

³Grand Accélérateur National d'Ions Lourds (GANIL), 14076 Caen Cedex 5, France

⁴STFC ISIS Pulsed Spallation Neutron and Muon Facility, Rutherford Appleton Laboratory, Harwell OX11 0QX, United Kingdom

^{a)} Author to whom correspondence should be addressed: ville.a.toivanen@jyu.fi

ABSTRACT

Electron Cyclotron Resonance (ECR) ion source plasmas are prone to kinetic instabilities. The onset of the instabilities manifests as emission of microwaves, bursts of electrons expelled from the plasma volume, and the collapse of the extracted highly charged ion (HCI) currents. Consequently, the instabilities limit the HCI performance of ECR ion sources by limiting the parameter space available for ion source optimization. Previous studies have shown that the transition from stable to unstable plasma regime is strongly influenced by the magnetic field structure, especially the minimum field value inside the magnetic trap (B_{\min}). This work focuses to study the role of the magnetic confinement on the onset of the kinetic instabilities by probing the influence of the injection and extraction mirror field variation on the instability threshold. The experiments have been performed with a room-temperature 14.5 GHz ECR ion source with an axially movable middle coil that provides flexible control over the axial field profile and especially the B_{\min} , which was used to quantify the variation in the instability threshold. The experimental results show that variation of the extraction field B_{ext} , which defines the weakest magnetic mirror, correlates systematically with the variation of the instability threshold; decreasing the B_{ext} allows higher threshold B_{\min} . The result demonstrates the importance of electron confinement and losses on the plasma stability. The connection between the weakest mirror field and the onset of instabilities is discussed taking into account the variation of magnetic field gradient and resonance plasma volume.

Published under an exclusive license by AIP Publishing. <https://doi.org/10.1063/5.0069638>

I. INTRODUCTION

Kinetic instabilities are found in various types of space and laboratory plasmas^{1–11} characterized by anisotropic electron energy distribution (EED) and run-away hot electron population. It has been shown experimentally that such non-linear phenomena affect the plasma confinement in minimum-B quadrupole mirror machines^{12,13} and electron cyclotron resonance ion sources (ECRIS)¹⁴ with combined solenoid and sextupole fields. In the case of ECRIS, the appearance of the instabilities is accompanied by reduced currents of extracted high charge state ion beams,¹⁵ which is explained by the periodic particle losses shortening the cumulative ion confinement time, thus disturbing the production of high charge state ions through stepwise ionization.

The instability is triggered by the stored electron energy accumulated¹⁶ into the anisotropic EED with $v_{\perp} \gg v_{\parallel}$ (with respect to the

confining magnetic field) and a (local) positive slope of the EED, i.e., $\frac{df(E)}{dE} > 0$. The threshold between stable and unstable plasma regimes is affected by electron heating and electron losses implying that the transition into the unstable maser regime is determined by the microwave power, neutral gas density and most importantly the magnetic field. It has been experimentally shown that in terms of the instability threshold the most influential magnetic field parameter of an ECRIS, operated with a single frequency i.e., constant B_{ECR} , is the value of the magnetic field minimum B_{\min} .^{17,18} When the ratio B_{\min}/B_{ECR} , where B_{ECR} is the cold electron resonance field satisfying the resonance condition with the plasma heating microwave frequency $\omega_{\text{RF}} = \frac{eB_{\text{ECR}}}{m_e}$, exceeds a certain value, kinetic instabilities emerge. Hence, it has been argued¹⁹ that the transition from stable to unstable plasma regime could explain the rule-of-thumb in ECRIS design, derived from the semi-empirical scaling laws²⁰ (see also references therein), stating that

$B_{\min}/B_{\text{ECR}} \leq 0.8$. Furthermore, it has been shown that the absolute value of B_{\min} correlates with the spectral temperature of plasma bremsstrahlung emission,²¹ which indicates that it is the most influential parameter affecting the plasma energy content $n_e \langle E_e \rangle$.

In the pulse-periodic instability regime, the build-up and sudden release of the plasma energy content alternate in periodic cycle leading to burst of microwaves, electrons, and ions from the plasma¹⁴ whereas it has been recently demonstrated²² that the turbulent regime can be controlled by carefully tuning the ECRIS into a continuous plasma maser mode characterized by quasi-CW emission of microwaves and enhanced fluxes of electrons and highly charged ions. In other words, it has been demonstrated that the magnitude and repetition rate of individual instability events is affected by the particle loss rate, not only the electron heating rate. This leads to the hypothesis that the instability threshold, i.e., the transition from stable to pulse-periodic instability regime, can be controlled by adjusting the fluxes of hot electrons determined by the RF scattering rate and mirror ratios of the axial and radial loss cones as discussed by Li *et al.*¹⁸ The magnetic field of modern ECR ion sources is designed on the basis of semi-empirical scaling laws setting desired values for the injection, radial, and extraction fields, i.e., $B_{\text{inj}} > 4B_{\text{ECR}}$, $B_{\text{rad}} > 2B_{\text{ECR}}$ and $B_{\text{ext}} \approx 0.9B_{\text{rad}}$.²⁰ Therefore, the scaling laws imply that the weakest magnetic mirror defining the *global loss cone* in $(v_{\parallel}, v_{\perp})$ -phase space is the extraction field. It has been shown that the electron flux escaping through the extraction aperture (mirror) of an ECRIS can be increased by more than a factor of two by decreasing the extraction field B_{ext} by 15%,^{23,24} which suggests that the total electron loss rate and/or the distribution of electron losses can be controlled by adjusting the weakest mirror. Based on the field topology and experimental evidence on electron losses it is argued that the extraction field could presumably affect the instability threshold, i.e., the exact B_{\min}/B_{ECR} -ratio at which instabilities appear. This paper describes experiments, conducted with a room-temperature 14.5 GHz ECRIS, probing the influence of the injection and extraction fields on the B_{\min} threshold of the instabilities. Following the previous arguments, it is expected that the impact of the injection field variation on the instability threshold is much weaker than the variation of the extraction field, arising from the high $B_{\text{inj}}/B_{\text{ext}}$ ratio and how the axial losses are consequently directed mainly toward the extraction.

It is noted here that the condition that the extraction field is the weakest mirror is not necessary fulfilled for every ECR ion source, as it depends on the details of the ion source magnetic design, especially the hexapole magnet structure and the solenoid coils which provide the radial and axial confinement, respectively. In a minimum- B structure, the radial magnetic field at the chamber wall B_{rad} is not a constant set only by the hexapole; the axial coils generate a radial magnetic field component which can locally oppose the hexapole radial field along the poles of the hexapole. Depending on the ECRIS design, the local field at wall can be reduced by 10–20 % by this effect.²⁵ Hence, even with the condition $B_{\text{ext}} \approx 0.9B_{\text{rad}}$ seemingly fulfilled when only the hexapole field is considered, in some cases the weakest magnetic mirror can still be at the radial wall.

The paper is organized as follows: the experimental setup and procedure are described in detail in Sec. II. The experimental results targeting to determine the relation between the axial mirror fields and the onset of plasma instabilities are presented in Sec. III, followed by a discussion in Sec. IV where we also present an outlook on how the

experimental findings accompanied by earlier results could guide the ECRIS design in the future.

II. EXPERIMENTAL SETUP AND PROCEDURE

The effect of various magnetic field parameters on the maser-type instability could be best studied with superconducting ECR ion sources where the field strength and topology can be adjusted more than with room-temperature ion sources. On the other hand, the power density (microwave power/volume enclosed by the cold electron ECR zone) is typically higher in room-temperature sources and varies less with the magnetic field adjustments, which alleviates the trouble of multiple source parameters affecting the data. In both source types the instability experiments, where the magnetic mirrors are adjusted, are complicated by the fact that changing the currents of the large bore solenoid coils not only affects the mirror field, e.g., B_{ext} , but also the distribution of magnetic field gradient on the resonance surface, plasma volume enclosed by the resonance zone and distance between the resonance zone and magnetic mirror, all of them potentially acting on the EED.

The GTS (Grenoble Test Source) ECRIS²⁶ was chosen for the study of comparing the importance of injection and extraction fields on the B_{\min} -threshold of the instability as it is one of the most flexible room-temperature ECRISs in terms of adjusting the field profile. This is largely owing to the construction of three solenoid coils with the middle coil being axially movable. In addition, the GTS Halbach-style hexapole provides a relatively high radial field of $B_{\text{rad}} = 1.2$ T at the poles on the plasma chamber wall, which helps to ensure that the weakest magnetic mirror is located at the source extraction (see the discussion at the end of this section). GTS was originally developed by CEA Grenoble and it has been operated at GANIL (Grand Accélérateur National d'Ions Lourds) since 2009. The source, currently working with 14.5 GHz plasma heating frequency, delivers multiply charged heavy ion beams for the low energy physics experiments of the ARIBE (Accélérateurs pour les Recherches Interdisciplinaires avec les Ions de Basse Energie) facility. The mechanical configuration of GTS at the time of the experiments discussed in this paper is presented in Fig. 1.

During 2016–2018 a number of refurbishments and upgrades were implemented to GTS in order to improve its performance.²⁷ Among these a new middle coil was installed between the main injection and extraction coils to provide more flexibility and control for adjusting the magnetic confinement of the ion source plasma. The middle coil axial location can be varied 28.5 mm from the geometric center position between the main coils toward the injection or 26.5 mm toward the extraction side of the source (see Fig. 2). The movement is limited by the mechanical construction of the middle coil support and the iron yokes of the injection and extraction coils. Three middle coil positions were used in the experiments; (1) the geometric axial center between the injection and the extraction coils (coinciding with the hexapole mid-plane, called later *center position*), (2) the coil set all the way toward the injection (*injection position*) and (3) the coil set all the way toward the extraction (*extraction position*). During this campaign, the middle coil polarity was set to be the same as the injection and extraction coils. In this configuration increase in the middle coil current increases the B_{\min} . An example of the resulting axial magnetic field profiles with the three different middle coil positions is presented in Fig. 3. In all the presented cases the injection,

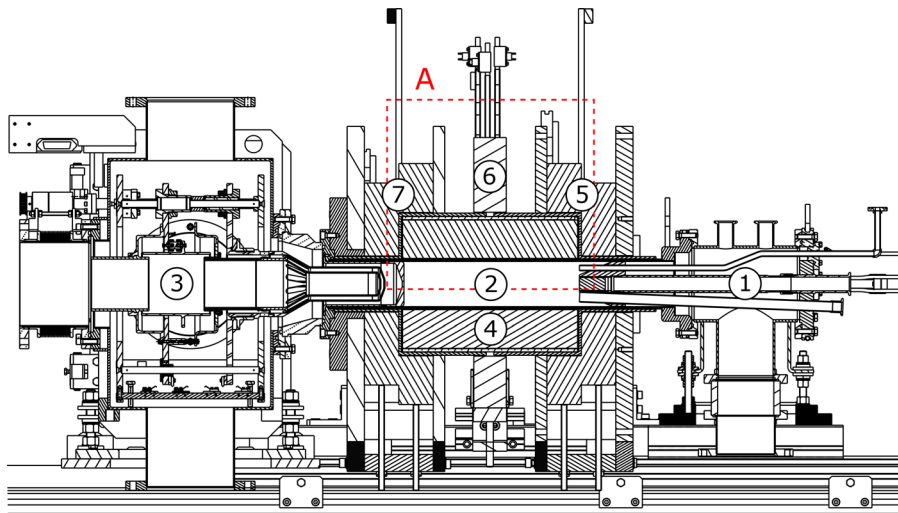


FIG. 1. A schematic of the GTS ECR ion source. The main components of the source include the injection system for microwave and gas delivery (1), the plasma chamber (2) and the beam extraction system comprising of a puller electrode and an einzel lens (3). The magnetic structure consists of a hexapole magnet (4) and the injection, the middle and the extraction coils (5, 6, and 7). The injection and extraction coils are divided into two separate pancake structures with different inner and outer radii. The section marked with (a) is shown in Fig. 2 to present the different positions of the middle coil.

middle and extraction coil currents are kept at 950, 330, and 950 A, respectively. As is seen in the figure, moving the middle coil between the two extreme positions (injection and extraction) shifts the axial location of B_{\min} about 5 mm (approximately 4% of the axial length of the ECR surface for cold electrons). Varying the middle coil position has also a minor effect on the extraction and injection mirror fields; moving the coil from the center position to the extraction or the injection positions causes a variation of about $\pm 0.6\%$ to B_{ext} and about $\pm 0.3\%$ to B_{inj} with these coil currents.

The experiments were performed with neon plasma. For the base tuning in stable plasma regime GTS was operated with 400 W microwave power, -100 V bias disk voltage and 10 kV extraction voltage. In order to allow flexibility for the magnetic field variation, the ion source coils were not optimized for the production of any specific ion charge state, i.e., the device was operated in a “plasma trap” rather than ion source mode. In the initial stable plasma tuning the middle coil was set to zero and both the injection and the extraction coil currents were set to 950 A, which corresponds to $B_{\text{inj}} = 1.97$ T, $B_{\text{ext}} = 0.97$ T, and $B_{\min} = 0.33$ T.

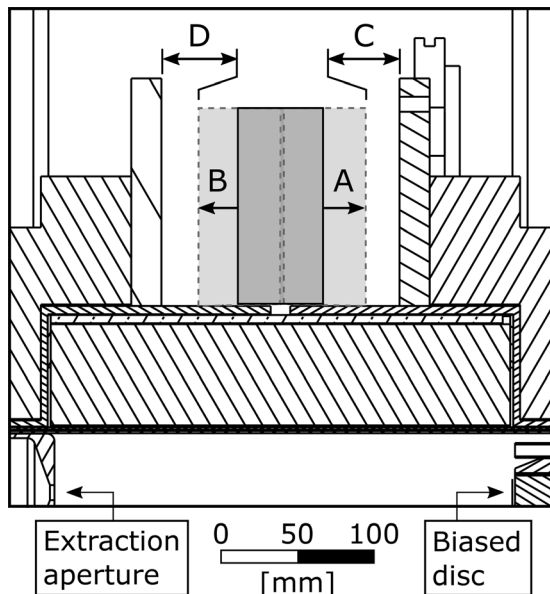


FIG. 2. The axial movement range of the GTS middle coil. The shown section is marked with (a) in Fig. 1. The coil can be moved from the geometric center position (i.e., hexapole mid-plane) 28.5 mm toward the injection (a) or 26.5 mm toward the extraction (b). In the injection position the coil is 22 mm from the iron yoke (c). In the extraction position the distance is 24 mm (d). The middle coil axial length is 57 mm. The extraction aperture and the biased disk are also indicated.

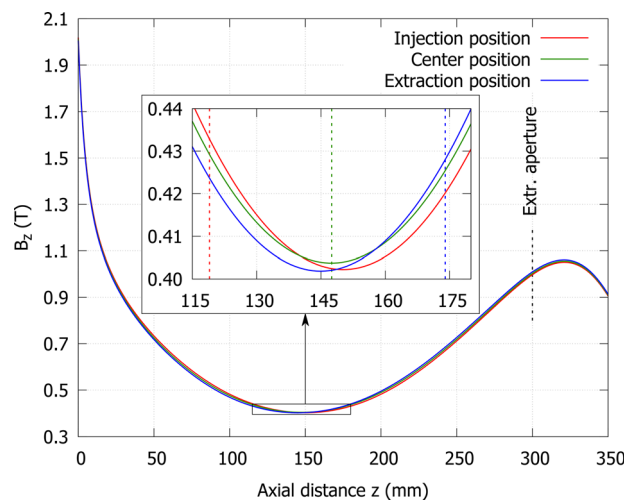


FIG. 3. Axial magnetic field profiles with the three different middle coil positions with the injection, middle and extraction coil currents set to 950, 330, and 950 A, respectively. The field profiles have been calculated with RADIA software^{28,29} using a 3D magnetic model of the GTS ECRIS. The axial location $z = 0$ mm is the surface of the biased disk at the injection end of the plasma chamber. The location of the extraction aperture, which defines the B_{ext} mirror field value for plasma confinement, is also indicated. The dashed vertical lines in the subplot indicate the axial locations of the middle coil mid-plane for the different coil positions.

The axial location for the B_{inj} is defined by the surface of the biased disk at the injection end of the plasma chamber and the B_{ext} location is defined by the extraction aperture (see Fig. 2). With the baseline settings the source produced a stable $10 \mu A$ beam of $^{20}Ne^{7+}$, which, being a high charge state, suffers notably when the plasma transitions into the unstable regime.

The occurrence of plasma instabilities was monitored with two BGO (bismuth germanate) x-ray detectors placed inside the axial radiation cones on the injection and the extraction sides of the ion source. In addition, the time evolution of the extracted beam current of $^{20}Ne^{7+}$ was monitored with an oscilloscope through a Keithley picoammeter connected to a Faraday cup downstream from the q/m analyzing magnet. The onset of the plasma instabilities was determined from the appearance of periodic x-ray bursts which correlate with the time structure of the extracted beam current, as discussed in the Introduction section. Examples of instability-induced x-ray and beam current signals, similar to those used here to detect the transition into unstable regime, can be found e.g., in Ref. 14.

Three sets of measurements were performed for each of the three middle coil positions. First, the injection coil current was varied in discrete steps from 950 to 1200 A (corresponding to B_{inj} variation from 1.97 to 2.17 T) while keeping the extraction coil constant at 950 A. For each injection coil current the B_{min} was increased by adjusting the middle coil current until the instability threshold was reached. Next, the injection coil current was kept constant at 950 A and the extraction coil current was varied from 950 to 1100 A (B_{ext} from 0.97 to 1.09 T), again finding the instability threshold B_{min} by changing the middle coil current. Finally, both the injection and the extraction coil currents were varied simultaneously from 950 to 1100 A, corresponding to $B_{inj} : 1.97 T \rightarrow 2.11 T$ and $B_{ext} : 0.97 T \rightarrow 1.09 T$, yet again finding the instability threshold B_{min} with the middle coil. In all the cases the injection and extraction coil currents were varied with fixed 25 A increments, resulting to data sets with linearly increasing B-field for the varied axial mirrors (B_{inj} , B_{ext} or both). The maximum coil currents were determined by the maximum output of the coil power supplies.

As discussed before, the radial component of the magnetic field generated by the injection, extraction and middle coils influences the total radial field on the plasma chamber walls, which causes a variation to the radial confinement when the coil currents and the middle coil position is varied. To quantify this effect, the total magnetic field on the plasma chamber wall was calculated for all the measured cases. The minimum total field on the poles of the hexapole magnet, which defines the radial mirror for the plasma confinement, was 10 – 22 % higher than B_{ext} in all the measured cases. This means that B_{ext} is always globally the weakest mirror.

III. EXPERIMENTAL RESULTS

The experimental results are presented in Figs. 4–6 for the three different middle coil positions. Each figure presents the threshold B_{min} for the plasma instability, above which the plasma is unstable, when either the injection, the extraction, or both of the coil currents are varied. The B_{inj} and B_{ext} range values presented in the figures correspond to the lowest and highest coil current values for each coil(s) sweep with the middle coil set at the B_{min} threshold value. The errors in the figures for the B_{min} threshold values are based on the size of the

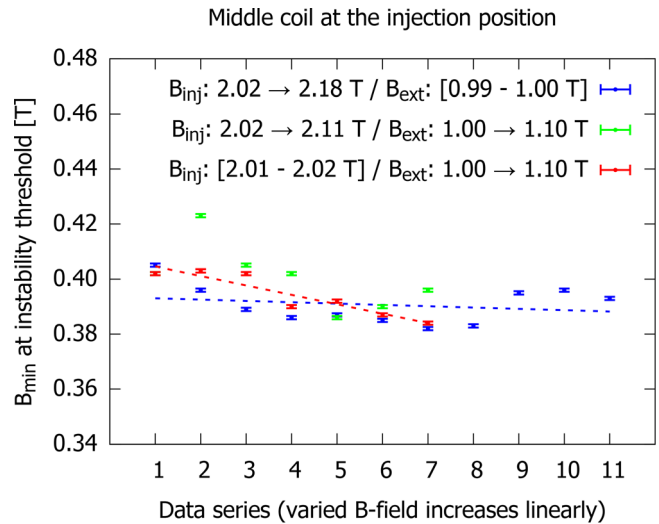


FIG. 4. B_{min} at the instability threshold with the middle coil at the injection position. Injection (blue), extraction (red) and both (green) coils were varied in steps in the different data series resulting to linear increase in the varied mirror fields over the ranges presented in the legend. The varied mirror field is indicated with an arrow in the legend between the first and the last field value of the sweep, while the range of field variation of the unaltered mirror (constant coil current) at the instability threshold B_{min} is presented in brackets. Trend lines of the instability threshold variation for the injection and the extraction coil sweeps are presented with dashed lines.

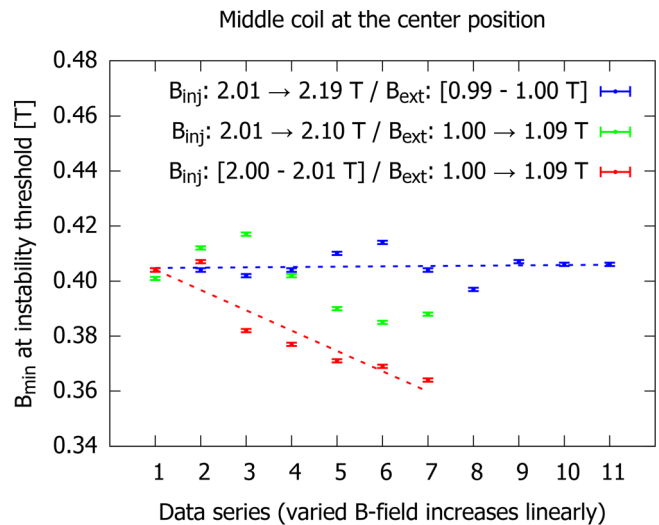


FIG. 5. B_{min} at the instability threshold with the middle coil at the center position. Injection (blue), extraction (red), and both (green) coils were varied in steps in the different data series resulting to linear increase in the varied mirror fields over the ranges presented in the legend. The varied mirror field is indicated with an arrow in the legend between the first and the last value of the sweep, while the range of field variation of the unaltered mirror (constant coil current) at the instability threshold B_{min} is presented in brackets. Trend lines of the instability threshold variation for the injection and the extraction coil sweeps are presented with dashed lines.

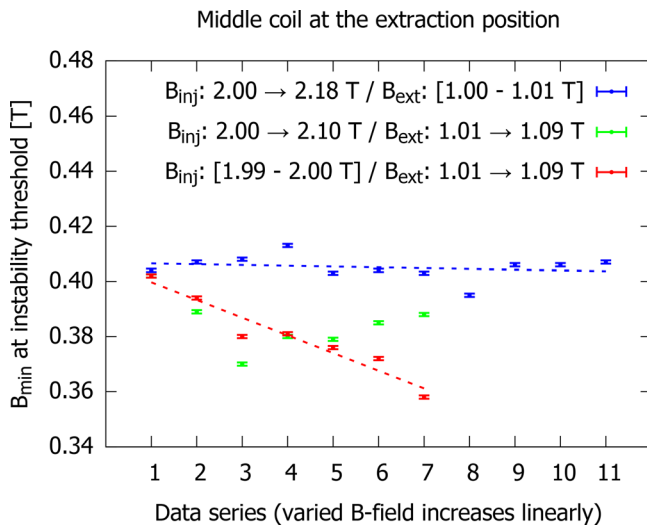


FIG. 6. B_{\min} at the instability threshold with the middle coil at the extraction position. Injection (blue), extraction (red), and both (green) coils were varied in steps in the different data series resulting to linear increase in the varied mirror fields over the ranges presented in the legend. The varied mirror field is indicated with an arrow in the legend between the first and the last field value of the sweep, while the range of field variation of the unaltered mirror (constant coil current) at the instability threshold B_{\min} is presented in brackets. Trend lines of the instability threshold variation for the injection and the extraction coil sweeps are presented with dashed lines.

current step in the middle coil (typically a few amperes) during which a clear transition from stable to unstable plasma regime was observed.

When the middle coil is set to injection position, see Fig. 4, varying the injection and extraction mirror fields has a relatively weak effect on the instability threshold value of B_{\min} . In all cases (either sweeping the injection, extraction, or both coils) a slight decrease in the B_{\min} threshold value is observed with increasing field values.

Figure 5 presents the results with the middle coil at the center location. Varying the injection field has practically no effect on the instability threshold B_{\min} -value, whereas increasing the extraction field results in a clear decrease in the B_{\min} threshold. A decrease in the threshold value is also observed when both the injection and the extraction fields are increased simultaneously.

Results with the middle coil at the extraction position are presented in Fig. 6. Like in the center position case, no systematic change of the B_{\min} threshold for the instabilities is observed with the variation of the injection field. When the extraction field or both the injection and the extraction fields are increased, a clear decrease in the instability threshold B_{\min} is found.

IV. DISCUSSION

The experimental results show that increasing the extraction mirror field strength leads to the instability threshold to occur at lower B_{\min} values, whereas the variation of the injection mirror has no or only a weak effect on the threshold. The observation implies that the EED of the confined electrons is affected more by the extraction than the injection field, which could be either due to the B-field acting on the electron confinement or on the ECR heating (e.g., by affecting the field gradient at the resonance). We argue that changing electron

confinement by the adjustment of the weakest magnetic mirror is the most likely explanation for the observed effect. It is emphasized that transition between stable and unstable regimes is dominated by B_{\min} , which appears to be the most influential magnetic field parameter acting on the anisotropy and hot tail of the EED, thus determining the instability threshold, whereas the control of electron losses and/or heating through the adjustment of the weakest mirror is a secondary effect offering the possibility to fine-tune the transition.

Distributions of fast electrons gaining their energy through ECR heating are usually unstable with respect to excitation of electromagnetic waves in the same frequency range.³⁰ The amplification of the excited EM-wave (observed as a burst of microwave emission) is determined by the balance between the instability growth and damping rates, which are defined by the electron energy and velocity distributions. These are in turn affected by the plasma density, power absorption and electron confinement in an inherently complex manner. It has been shown experimentally^{23,24} that adjusting B_{ext} by 10% (similar to the experiment reported here) has a significant impact on the electron flux escaping the ion source through the extraction aperture. This is arguably due to the mirror ratio $R = \frac{B_{\text{max}}}{B_{\text{min}}}$ of the magnetic configuration affecting the escape probability p of electrons as $p = a(1 - \sqrt{1 - \frac{1}{R}})$, where a is the isotropy factor of the electron velocity distribution ($a = 1$ for perfectly isotropic EVD and $a < 1$ when $v_{\perp} > v_{\parallel}$). The above proportionality implies that if B_{ext} is increased from 1.0 to 1.1 T with B_{\min} of 0.4 T, the probability for electrons to escape through the extraction mirror decreases by approximately 10%, i.e., more energy is accumulated in the EED, which makes the instabilities more likely to appear. The stability can be restored by lowering B_{\min} , which is the most influential magnetic field parameter affecting the appearance of the instabilities. The fact that lowering B_{ext} allows higher B_{\min} at the instability threshold could make it possible to optimize the high charge state beam currents, which tend to increase with B_{\min} until the transition from stable to unstable regime occurs.¹⁹

Thus far, we have only discussed how the extraction mirror (B_{ext}) presumably affects the instability threshold B_{\min} through electron confinement. However, since the EED is affected not only by the electron confinement but also by the electron heating characteristics, both aspects discussed from experimental standpoint e.g., in Ref. 18, we need to consider how the magnetic field adjustment in our experiment is likely to affect the electron heating and plasma energy content.

The volumetric power absorption (P_{abs}) by the electrons in the absence of collisions is inversely proportional to the difference between the resonance field B_{ECR} and the local magnetic field B to the square as $\langle P_{\text{abs}} \rangle \propto 1/(B_{\text{ECR}} - B)^2$ as discussed in Ref. 31. Therefore, the electron energy gain in each resonance crossing depends strongly on the parallel magnetic field gradient at the resonance, $\frac{\partial B}{\partial z} \cdot \nabla B$, as discussed by many authors.^{31–33} We have calculated the average parallel gradient $\langle \nabla B_{\text{ECR}} \rangle_{\parallel}$ on the (cold electron) ECR surface with the coil currents at the observed instability threshold. Figure 7 shows the average gradient as a function of B_{\min} at the instability threshold with various mid-coil positions when the extraction coil current is swept causing the extraction field (B_{ext}) to change from 1.0 to 1.1 T with the injection field remaining constant. It is seen that the average gradient increases with increasing B_{ext} with all mid-coil positions. Thus, following the argument that the electron heating rate decreases with increasing gradient, it could be expected that increasing B_{ext} would result in higher B_{\min} at

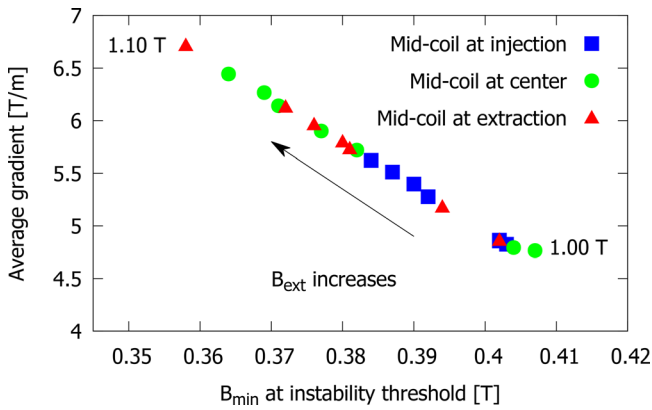


FIG. 7. The average magnetic field gradient parallel to the magnetic field on the (cold electron) resonance as a function of B_{\min} at the instability threshold with different middle coil position when the extraction coil current (B_{ext}) is varied keeping the injection coil current (B_{inj}) constant.

the instability threshold. The trend in Fig. 7 is exactly the opposite suggesting that the electron confinement (defined by the strength of the weakest mirror field, B_{ext} , in this case) overpowers the effect of the gradient determining the B_{\min} threshold value.

The spatial distribution of hot electrons in ECRIS plasmas has been studied both numerically and experimentally^{34–36} and it has been concluded that the majority of the plasma energy content is carried by the electron population in the dense plasmoid surrounded by the ECR surface. As the instabilities are driven by the local EED, it could be argued that the volume enclosed by the resonance zone therefore affects the B_{\min} at the instability threshold. Figure 8 shows the volume enclosed by the (cold electron) resonance as a function of B_{\min} at the instability threshold with various mid-coil positions when the extraction coil current is swept similar to Fig. 7. The volume increases with increasing B_{ext} with all mid-coil positions. If the instability threshold was to be determined by the volumetric effect, an opposite trend, i.e., increased energy density leading to lower B_{\min} threshold value, would be expected.

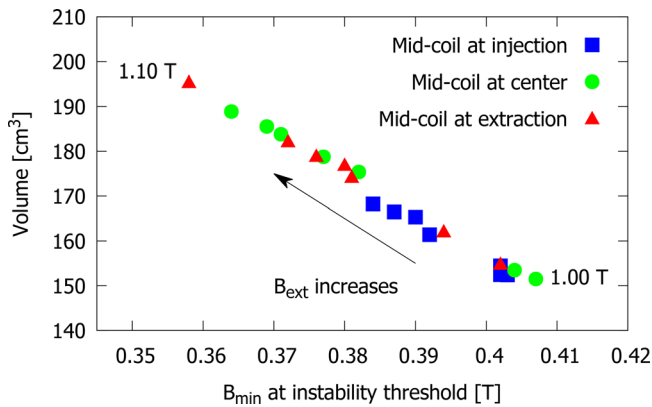


FIG. 8. The volume enclosed by the (cold electron) resonance zone as a function of B_{\min} at the instability threshold with different middle coil position when the extraction coil current (B_{ext}) is varied keeping the injection coil current (B_{inj}) constant.

Considering both, the gradient and volume effects, and concluding that neither one of them matches the experimental observation strengthens the argument that the electron confinement plays an important role in determining the transition between stable and unstable discharge regimes.

Previous studies¹⁴ have shown that the source potential (extraction voltage) also influences the instability threshold, and applying the potential shifts the threshold to lower B_{\min}/B_{ECR} values. This effect is not yet completely understood, but the source potential does also influence the axial electron confinement, as it creates an electrostatic barrier at the extraction which suppresses the axial electron losses toward this direction for electron energies below the limit set by the potential. For example, in the experiments presented here the source potential was set to 10 kV, which consequently stops the axial electron losses toward the extraction for electrons with energies below 10 keV. As a result, the electron losses are drastically reduced, impacting the properties of the confined electron population. This then affects the ion population in plasma, as has been shown with optical measurements of ECR plasma.³⁷

The connection between the electron confinement and the onset of the instabilities opens up the prospect of a more active control over the electron losses during ECRIS operation to suppress the plasma instabilities and optimize the source performance. In a typical ECRIS the adjustment of the magnetic system with the currents of large-bore coils impacts globally the field structure inside the plasma chamber, influencing both the plasma confinement and the plasma heating through the variation of the magnetic gradient and the plasma volume, as discussed above. However, because the instability transition can be argued to be especially sensitive to the strength of the weakest mirror, as the results presented here imply, a local modification of the B -field near this position with an additional localized magnetic system could be used to control the electron losses from the plasma without significantly disturbing the global magnetic field properties. Additionally, this would also enhance the ion flux from the plasma toward extraction and beam formation. In effect, this approach could provide an additional “tuning knob” for the instabilities without restricting the parameter space for magnetic field optimization in terms of ion production. One option to realize this local control could be to install an additional compact coil close to the extraction mirror. Studies with plasma electrode collar structures^{38,39} have shown that inside an ECRIS plasma chamber there exists an amount of space around the extraction aperture which can be utilized without negatively impacting the source performance. A compact coil structure fixed in this location would be well positioned to provide a localized and adjustable modification to the extraction mirror field to control the electron losses. It is acknowledged that for practical reasons designing such a compact coil to operate continuously in vacuum with sufficiently high currents to provide significant impact on the magnetic field could be challenging. However, such a structure could provide benefits also when operated in pulsed mode, which simplifies the design. In this mode it could be used also to enhance extracted high charge state ion currents in afterglow operation. The PUMAEX (Pulsed Magnetic Extraction) experiments^{40,41} have shown that a pulsed magnetic coil structure located at the extraction end of an ECRIS plasma chamber can be used to direct the plasma flux toward the beam extraction by temporarily decreasing the magnetic confinement in that region. Combining this approach with pulsed afterglow operation, the local control over the

magnetic confinement would make it possible to keep the mirror fields high during the steady state of the plasma heating cycle to accumulate a large population of highly charged ions in the plasma by mitigating the ion losses during this phase. At the cutoff of the microwaves the magnetic trap could then be emptied more efficiently by simultaneously “opening” the trap toward the extraction by a local modification of the magnetic field, providing a further enhancement of the highly charged ion currents during the afterglow burst.

Instead of a coil, the local modification of the magnetic confinement could also be realized with movable permanent magnet (or soft iron) structures to allow local adjustment of the electron losses. Although potentially simpler than the coil method, careful magnetic design would still be required to optimize the design. The main downside of these approaches is that unlike a coil, once the modifications are installed, their magnetic influence can not be easily switched off completely.

ACKNOWLEDGMENTS

This work has been supported by the Academy of Finland Project funding (No. 315855) and University of Grenoble Alpes under the EMERGENCE program.

AUTHOR DECLARATIONS

Conflict of interest

The authors have no conflicts to disclose.

DATA AVAILABILITY

The data that supports the findings of this study are available within the article.

REFERENCES

- ¹R. Thorne, “Radiation belt dynamics: The importance of wave–particle interaction,” *Geophys. Res. Lett.* **37**, L22107, <https://doi.org/10.1029/2010GL044990> (2010).
- ²D. Gurnett, “The Earth as a radio source: Terrestrial kilometric radiation,” *J. Geophys. Res.* **79**, 4227–4238, <https://doi.org/10.1029/JA079i028p04227> (1974).
- ³M. Panchenko, H. Rucker, and W. Farrell, “Periodic bursts of Jovian non-Io decametric radio emission,” *Planet. Space Sci.* **77**, 3–11 (2013).
- ⁴D. Melrose and G. Dulk, “Electron-cyclotron masers as the source of certain solar and stellar radio bursts,” *Astrophys. J.* **259**, 844–858 (1982).
- ⁵J. Nichols, M. Burleigh, S. Casewell, S. Cowley, G. Wynn, J. Clarke, and A. West, “Origen of electron cyclotron maser induced radio emissions at ultra-cool dwarfs: Magnetosphere-ionosphere coupling currents,” *Astrophys. J.* **760**, 1–9 (2012).
- ⁶W. Ard, R. Dandl, and R. Stetson, “Observations of instabilities in electron-cyclotron plasmas,” *Phys. Fluids* **9**, 1498 (1966).
- ⁷V. Alikae, V. Glagolev, and S. Morozov, “Anisotropic instability in a hot electron plasma, contained in an adiabatic trap,” *Plasma Phys.* **10**, 753–774 (1968).
- ⁸A. Shalashov and E. Suvorov, “On cyclotron emission from toroidal plasmas near the ECR heating frequency,” *Plasma Phys. Controlled Fusion* **45**, 1779 (2003).
- ⁹J. Cook, R. Dendy, and S. Chapman, “Particle-in-cell simulations of the magnetoacoustic cyclotron instability of fusion-born alpha-particles in tokamak plasmas,” *Plasma Phys. Controlled Fusion* **55**, 065003 (2013).
- ¹⁰R. Post and W. Perkins, “Velocity-space plasma instabilities observed in a mirror machine,” *Phys. Rev. Lett.* **6**, 85 (1961).
- ¹¹A. Demekhov and V. Trakhtengerts, “Several questions on radiation dynamics in magnetic plasma traps,” *Radiophys. Quantum Electron.* **29**, 848–857 (1986).
- ¹²R. Garner, M. Mauel, S. Hokin, R. Post, and D. Smatlak, “Warm electron-driven whistler instability in an electron-cyclotron-resonance heated, mirror-confined plasma,” *Phys. Rev. Lett.* **59**, 1821 (1987).
- ¹³R. Garner, M. Mauel, S. Hokin, R. Post, and D. Smatlak, “Whistler instability in an electron-cyclotron-resonance-heated, mirror-confined plasma,” *Phys. Fluids B* **2**, 242 (1990).
- ¹⁴O. Tarvainen, I. Izotov, D. Mansfeld, V. Skalyga, S. Golubev, T. Kalvas, H. Koivisto, J. Komppula, R. Kronholm, J. Laulainen, and V. Toivanen, “Beam current oscillations driven by cyclotron instabilities in a minimum-B electron cyclotron resonance ion source plasma,” *Plasma Sources Sci. Technol.* **23**, 025020 (2014).
- ¹⁵O. Tarvainen, T. Kalvas, H. Koivisto, J. Komppula, R. Kronholm, J. Laulainen, I. Izotov, D. Mansfeld, V. Skalyga, V. Toivanen, and G. Machicoane, “Limitation of the ecris performance by kinetic plasma instabilities (invited),” *Rev. Sci. Instrum.* **87**, 02A703 (2016).
- ¹⁶A. Shalashov, S. Golubev, E. Gospodchikov, D. Mansfeld, and M. Viktorov, “Interpretation of complex patterns observed in the electron-cyclotron instability of a mirror confined plasma produced by an ECR discharge,” *Plasma Phys. Controlled Fusion* **54**, 085023 (2012).
- ¹⁷I. Izotov, A. Shalashov, V. Skalyga, E. Gospodchikov, O. Tarvainen, V. Mironov, H. Koivisto, R. Kronholm, V. Toivanen, and B. Bhaskar, “The role of radio frequency scattering in high-energy electron losses from minimum-B ECR ion source,” *Plasma Phys. Controlled Fusion* **63**, 045007 (2021).
- ¹⁸J. Li, L. Li, B. Bhaskar, V. Toivanen, O. Tarvainen, D. Hitz, L. Li, W. Lu, H. Koivisto, T. Thuillier, J. Guo, X. Zhang, H. Zhao, L. Sun, and H. Zhao, “Effects of magnetic configuration on hot electrons in a minimum-B ECR plasma,” *Plasma Phys. Controlled Fusion* **62**, 095015 (2020).
- ¹⁹O. Tarvainen, J. Laulainen, J. Komppula, R. Kronholm, T. Kalvas, H. Koivisto, I. Izotov, D. Mansfeld, and V. Skalyga, “Limitations of electron cyclotron resonance ion source performances set by kinetic plasma instabilities,” *Rev. Sci. Instrum.* **86**, 023301 (2015).
- ²⁰D. Hitz, A. Girard, G. Melin, S. Gammino, G. Ciavola, and L. Celona, “Results and interpretation of high frequency experiments at 28 GHz in ECR ion sources, future prospects,” *Rev. Sci. Instrum.* **73**, 509–512 (2002).
- ²¹J. Benitez, C. Lyneis, L. Phair, D. Todd, and D. Xie, “Dependence of the bremsstrahlung spectral temperature in minimum-B electron cyclotron resonance ion sources, future prospects,” *IEEE Trans. Plasma Sci.* **45**, 1746–1754 (2017).
- ²²V. Skalyga, I. Izotov, A. Shalashov, E. Gospodchikov, E. Kiseleva, O. Tarvainen, H. Koivisto, and V. Toivanen, “Controlled turbulence regime of electron cyclotron resonance ion source for improved multicharged ion performance,” *J. Phys. D: Appl. Phys.* **54**, 385201 (2021).
- ²³I. Izotov, O. Tarvainen, V. Skalyga, D. Mansfeld, T. Kalvas, H. Koivisto, and R. Kronholm, “Measurement of the energy distribution of electrons escaping minimum-B ECR plasmas,” *Plasma Sources Sci. Technol.* **27**, 025012 (2018).
- ²⁴B. S. Bhaskar, H. Koivisto, O. Tarvainen, T. Thuillier, V. Toivanen, T. Kalvas, I. Izotov, V. Skalyga, R. Kronholm, and M. Martinen, “Correlation of bremsstrahlung and energy distribution of escaping electrons to study the dynamics of magnetically confined plasma,” *Plasma Phys. Controlled Fusion* **63**, 095010 (2021).
- ²⁵T. Thuillier, J. Angot, J. Y. Benitez, A. Hodgkinson, C. M. Lyneis, D. S. Todd, and D. Z. Xie, “Investigation on the electron flux to the wall in the VENUS ion source,” *Rev. Sci. Instrum.* **87**, 02A736 (2016).
- ²⁶D. Hitz, D. Cormier, J. Mathonnet, A. Girard, G. Melin, F. Lansaque, K. Serebrennikov, and L. Sun, “Grenoble test source GTS: A multipurpose room temperature ECRIS,” in *Proceedings of the 15th International Workshop on Electron Cyclotron Resonance Ion Sources*, Jyväskylä, Finland (2002).
- ²⁷V. Toivanen, C. Barué, C. Feierstein, P. Jardin, F. Lemagnen, L. Maunoury, F. Noury, and P. Rousseau, “Upgrade of the GTS electron cyclotron resonance ion source at GANIL,” *AIP Conf. Proc.* **2011**, 040008 (2018).
- ²⁸P. Elleaume, O. Chubar, and J. Chavanne, “Computing 3d magnetic fields from insertion devices,” in *Proceedings of the 1997 Particle Accelerator Conference (Cat. No. 97CH36167)*, Vancouver, Canada (IEEE, 1997), pp. 3509–3511.
- ²⁹See <http://www.esrf.eu/Accelerators/Groups/InsertionDevices/Software/Radia> for “Radia Software Website” (last accessed October 21, 2021).
- ³⁰A. Shalashov, E. Gospodchikov, and I. Izotov, “Electron-cyclotron heating and kinetic instabilities of a mirror-confined plasma: The quasilinear theory revised,” *Plasma Phys. Controlled Fusion* **62**, 065005 (2020).
- ³¹M. Williamson, A. Lichtenberg, and M. Lieberman, “Self-consistent electron cyclotron resonance absorption in a plasma with varying parameters,” *J. Appl. Phys.* **72**, 3924 (1992).

- ³²E. Canobbio, "Gyroresonant particle acceleration in a non-uniform magnetostatic field," *Nucl. Fusion* **9**, 27 (1969).
- ³³S. Gammino, D. Mascali, L. Celona, F. Maimone, and G. Ciavola, "Considerations on the role of the magnetic field gradient in ECR ion sources and build-up of hot electron component," *Plasma Sources Sci. Technol.* **18**, 045016 (2009).
- ³⁴D. Mascali, L. Neri, L. Celona, G. Castro, G. Torrisi, S. Gammino, G. Sorbello, and G. Ciavola, "A double-layer based model of ion confinement in electron cyclotron resonance ion source," *Rev. Sci. Instrum.* **85**, 02A511 (2014).
- ³⁵V. Mironov, S. Bogomolov, A. Bondarchenko, A. Efremov, V. Loginov, and D. Pugachev, "Spatial distributions of plasma potential and density in electron cyclotron resonance ion source," *Plasma Sources Sci. Technol.* **29**, 065010 (2020).
- ³⁶R. Rácz, S. Biri, J. Pálincás, D. Mascali, G. Castro, C. Caliri, L. Neri, F. Romano, and S. Gammino, "Structural information on the ECR plasma by x-ray imaging," in Proceedings of the 22nd International Workshop on Electron Cyclotron Resonance Ion Sources, Busan, Korea (2016).
- ³⁷R. Kronholm, T. Kalvas, H. Koivisto, and O. Tarvainen, "Spectroscopic method to study low charge state ion and cold electron population in ECRIS," *Rev. Sci. Instrum.* **89**, 043506 (2018).
- ³⁸V. Toivanen, O. Tarvainen, J. Komppula, and H. Koivisto, "The effect of plasma electrode collar structure on the performance of the JYFL 14 GHz electron cyclotron resonance ion source," *Nucl. Instrum. Methods Phys. Res., Sect. A* **726**, 41–46 (2013).
- ³⁹V. Mironov, J. Beijers, H. Kremers, J. Mulder, S. Saminathan, and S. Brandenburg, "ECRIS development at KVI," in Proceedings of the 19th International Conference on Cyclotrons and Their Applications, Lanzhou, China (2010).
- ⁴⁰L. Müller, A. Heinen, H. Ortjohann, and H. Andrä, "Magnetic pulsed extraction of highly charged ions from a plateau ECRIS," *Rev. Sci. Instrum.* **73**, 1140 (2002).
- ⁴¹L. Müller, B. Albers, A. Heinen, M. Kahnt, L. Nowack, H. Ortjohann, A. Täschner, C. Vitt, S. Wolosin, and H. Andrä, "The new MÜNSTER 18 GHz plateau-ECRIS," in Proceedings of the 15th International Workshop on Electron Cyclotron Resonance Ion Sources, Jyväskylä, Finland (2002).